

# Compact object coalescence rate estimation from short gamma-ray burst observations

Carlo Enrico Petrillo

Dipartimento di Scienze Fisiche, Università di Napoli “Federico II,”  
Compl. Univ. Monte S. Angelo, Ed. N, Via Cinthia, I-80126 Napoli, Italy

Alexander Dietz

Department of Physics and Astronomy, The University of Mississippi  
University, MS 38677-1848 USA

Marco Cavaglia

Department of Physics and Astronomy, The University of Mississippi  
University, MS 38677-1848, USA

Received \_\_\_\_\_; accepted \_\_\_\_\_

## ABSTRACT

Recent observational and theoretical results suggest that Short-duration Gamma-Ray Bursts (SGRBs) are originated by the merger of compact binary systems of two neutron stars or a neutron star and a black hole. The observation of SGRBs with known redshifts allows astronomers to infer the merger rate of these systems in the local universe. We use data from the SWIFT satellite to estimate this rate to be in the range  $\sim 500\text{-}1500 \text{ Gpc}^{-3}\text{yr}^{-1}$ . This result is consistent with earlier published results which were obtained through alternative approaches. We estimate the number of coincident observations of gravitational-wave signals with SGRBs in the advanced gravitational-wave detector era. By assuming that all SGRBs are created by neutron star-neutron star (neutron star-black hole) mergers, we estimate the expected rate of coincident observations to be in the range  $\simeq 0.2$  to  $1$  ( $\simeq 1$  to  $3$ )  $\text{yr}^{-1}$ .

*Subject headings:* gamma-ray bursts: general, gravitational waves

## 1. Introduction

Short-duration Gamma-Ray Bursts (SGRBs) are some of the most powerful explosions detected in the universe, releasing intensive bursts of high-energy gamma rays with a peak duration shorter than two seconds (Kouveliotou et al. 1993). The most commonly accepted explanation of their origin is a system of two compact objects, either two Neutron Stars (NS-NS) or a Neutron Star and a Black Hole (NS-BH) coalescing into a black hole (Eichler et al. 1989; Narayan et al. 1992; Piro 2005; Rezzolla et al. 2011). Because of the emission of Gravitational Waves (GWs) during the latest phases of the binary evolution, these objects are one of the primary sources for the next generation of ground-based GW detectors such as Advanced LIGO (Smith 2009) and Advanced Virgo (Acernese et al. 2008). Direct detection of a GW signal from a compact binary coalescing system would allow astronomers to gain valuable information on the astrophysics of compact objects, for example the NS equation of state (Flanagan & Hinderer 2008; Read et al. 2009), as well as probe fundamental physics by testing the Lorentz invariance principle (Ellis et al. 2006) and general relativity in the strong-field regime (Will 2005), or by setting limits on the graviton mass (Stavridis & Will 2009; Keppel & Ajith 2010). Direct detection of a GW signal in coincidence with a GRB optical counterpart could provide additional insights on astrophysics and even cosmology. The measure of the redshift of a GRB in coincidence with a GW detection could allow astronomers to directly determine the distance of the system (see, e.g., Nissanke et al. (2010) and references therein). Coincident detections could also significantly improve the determination of the Hubble parameter by GW observations (Dalal et al. 2006; Del Pozzo 2011).

In this context, it is crucial to have reliable estimates of the local merger rate of compact

objects and the number of expected coincident GW-GRB observations in the advanced GW detector era. In this paper we present a simple estimate of these quantities by using GRB data from SWIFT observations <sup>1</sup>. In order to avoid selective bias, we calculate the number of expected coincident observations by restricting the sample of SWIFT data to observations with determined redshift and certain association to an optical counterpart. In contrast to a previous study by one of the authors (Dietz 2011), we also include the observed GRB luminosities in the analysis.

The paper is organized as follows. In Section 2 we define the SWIFT data sample and discuss the theoretical model which is used to fit the observations. In Section 3 we present the results and compare them to other published rate estimates. The Appendix contains details on the rate functions used in the analysis.

## 2. SWIFT data sample and fitting model

We restrict our analysis to a set of GRBs with reliable redshift measurement, i.e., to GRBs that can be associated to a galaxy of known spectroscopic redshift with a high probability of being the host galaxy of the GRB. We omit from the analysis GRBs without an observed optical afterglow and GRBs that are not associated with a host galaxy within the error-circle of the observation. This allows us to remove any instrumental bias with respect to GRBs detected by other missions. Table 1 shows the list of the 14 SWIFT GRBs that pass our selection criteria.

---

<sup>1</sup><http://heasarc.gsfc.nasa.gov/docs/swift/swiftsc.html>

The luminosity of these SGRBs can be computed using their redshift and fluence information. The fluence  $S$  is divided by the SGRB duration to estimate the flux  $F$  in the relevant frame for the detection threshold of the satellite (the observer frame). Since the observed fluence depends on the spectral properties of the source and the energy response of the detector (15 to 150 keV for the BAT instrument onboard SWIFT, see Barthelmy (2005)), and the observations are over cosmological distances, two identical sources at different distances may show a spectral shift and a change of fluence. Expressing the observed photon number spectrum with the Band function (Band et al. 1993), this spectral shift can be calculated as a function of the redshift (Cao et al. 2011). Since most SGRB sources have redshift smaller than  $z = 1$ , the effect of the spectral shift is less than 10% (Cao et al. 2011). This error is small compared to other statistical and systematical errors and will be neglected in our analysis. The apparent luminosity of the SGRB is

$$L = 4\pi d_L^2(z) F \simeq 4\pi d_L^2(z) \frac{S}{T_{90}}, \quad (1)$$

where  $d_L(z)$  is the luminosity distance for a given redshift  $z$ ,  $F$  is the mean flux,  $S$  is the measured fluence and  $T_{90}$  is the time over which the burst emits 90% of its total energy. Throughout this paper we consider a standard flat- $\Lambda$  cosmology with  $H_0 = 71 \text{ km s}^{-1}$ ,  $\Omega_M = 0.27$  and  $\Omega_\Lambda = 0.73$ . The left panel of Fig. 1 shows the distribution of the observed luminosities as a function of the redshift. The solid line indicates the approximate detector’s sensitivity threshold

$$d_{\max}(L) = \sqrt{\frac{L}{4\pi F_{\text{lim}}}}, \quad (2)$$

where the flux threshold is  $F_{\text{lim}} = 5 \times 10^{-9} \text{ erg s}^{-1} \text{ cm}^{-2}$  (Cao et al. 2011). The grey area in Fig. 1 defines the so-called *redshift desert*, a region between  $z \simeq 1$  and  $z \simeq 2$  where spectroscopic redshift determinations are difficult to obtain (Fiore et al. 2007). In

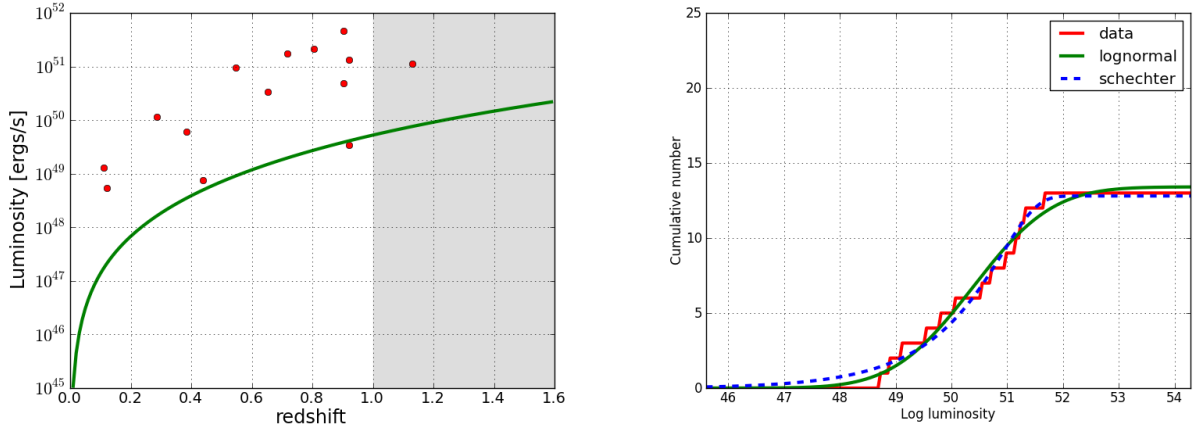


Fig. 1.— Left panel: Luminosity distribution of the 14 SGRBs which pass the analysis selection criteria as function of their redshift. The grey area represents the *redshift desert*. Our analysis is restricted to the 13 SGRBs with  $z < 1$ . Right panel: Cumulative distribution of the SGRBs as a function of luminosity (red), the lognormal function fit (green), and the Schechter function fit (dashed blue).

the following, we choose a conservative approach and further restrict our data sample to  $z < 1$ , leaving 13 data points for our analysis.

To determine the local merger rate, we fitted the sample with several, commonly-used luminosity functions (Dietz 2011; Chapman et al. 2008; Guetta & Stella 2008). The lognormal function and the Schechter function were found to provide acceptable fits. The cumulative distribution of the SGRBs as a function of the luminosity and the lognormal and Schechter functions are shown in Fig. 1. Since the lognormal fit is slightly better than the Schechter fit, we restrict our analysis to the lognormal luminosity function

$$\phi(L) \propto \frac{1}{L} \exp\left(-\frac{\log L - \log L_0}{2\sigma^2}\right), \quad (3)$$

where  $L_0$  is the mean (peak) value of the luminosity and  $\sigma$  is the width of the distribution. These two parameters are determined by fitting the function to the 13 SGRBs in the sample. For sake of simplicity, we do not consider evolutionary effects on the luminosity function. Although it is reasonable to assume that these effects are small compared to other statistical and systematical errors, some physical processes depend on the metallicity of the progenitors, which is a function of the redshift (Belczynski et al. 2010, 2011). The right panel of Fig. 1 shows the cumulative distribution of SGRBs as a function of luminosity and the lognormal fit in Eq. (3).

Since the fit is made on *observed* SGRBs, the luminosity function  $\phi'(L)$  must be rescaled to the volume where SWIFT is sensitive. Assuming an isotropic distribution of SGRBs, we write

$$\phi(L) \propto \phi'(L)/d_{\max}^3(L), \quad (4)$$

where  $d_{\max}^3(L)$  is the maximum luminosity distance where a SGRB can be detected by SWIFT. The number of observable SGRBs within a redshift distance  $z$  is

$$N'(z) = N_0 \int_0^z dz' \frac{R(z')}{1+z'} \frac{dV(z')}{dz'} \int_{L_{\min}(z')}^{\infty} \phi(L) dL, \quad (5)$$

where  $dV(z')/dz'$  is the comoving volume element and  $N_0$  is a normalization factor. The rate function  $R(z)$  describes the formation rate of the binary systems per comoving volume as a function of the redshift. Since a binary system of compact objects is formed from massive progenitor stars,  $R(z)$  may be assumed to follow the star formation rate. The time difference from the formation of the compact objects to the coalescence of the binary is likely on the order of the Gyr (Belczynski et al. 2006). Thus there is a significant delay with respect to the star formation rate. This is taken into account by using a delayed rate function in Eq. (5). Figure 2 shows different rate functions that are used in our

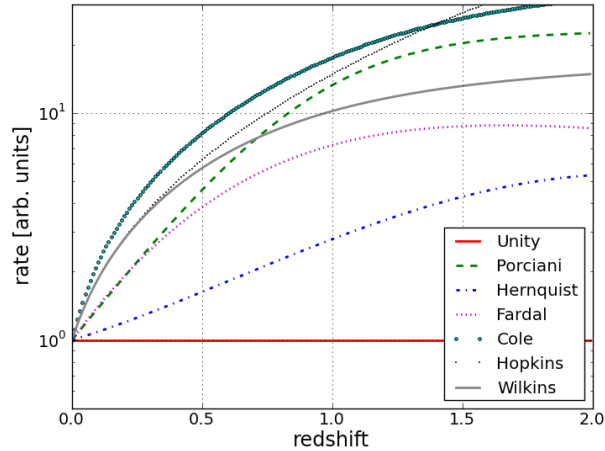


Fig. 2.— Different rate functions used in the analysis (see the Appendix for details). Note that the rate functions vary significantly even for redshift distances  $z < 1$ .

analysis. The Appendix contains explicit expressions and references.

Since Eq. (5) describes the number of SGRBs that may be potentially observed,  $N'(z)$  must be rescaled to fit the number of SGRBs used in the analysis. From 2005 through 2011 ( $T \simeq 6$  yr) SWIFT observed 46 SGRBs. (We neglect any downtime of the satellite due to technical issues or other constraints.) Thus  $N'(z)$  must be divided by the factor  $f_R = 14/46$ , with an estimated error of  $\sqrt{14}/46 \sim 10\%$ . The SWIFT field of view is about 1.4 sr (Barthelmy 2005), corresponding to a visible fraction of the sky approximately equal to  $f_{FOV} \simeq 10\%$ . Observations have shown that about 15% of all SGRBs may be created by Soft Gamma Repeaters (SGRs) (Nakar et al. 2006; Chapman et al. 2008). Since SGRs are typically less bright than ordinary SGRBs, events at larger redshifts might be composed mainly of SGRBs. If we assume that 85% of all SGRBs



are created by the merger of two compact objects, the factor  $f_{\text{SGR}} = 0.85$  yields a conservative limit on the merger rate. In order to create a relativistic outflow, a torus must be created around the newly formed black hole. Simulation and theoretical analyses show that the formation of a GRB depends on several parameters such as spin of the black hole, the mass ratio of the binary or the compactness of the neutron star (Pannarale et al. 2010; Rezzolla et al. 2011). Since these parameters are hard to generalize, we simply assume that all compact object mergers produce a GRB. GRBs are believed to emit their radiation in a collimated cone. The half-opening angle  $\theta$  defines the fraction of the sky where the burst can be seen,  $f_b = 1 - \cos \theta$ . The angle  $\theta$  is highly uncertain, especially in the case of SGRBs, as it depends on the model and the Lorentz factor of the outflow (Panaitescu & Kumar 2001). Measurements of SGRB half-opening angles range from a few degrees to over  $25^\circ$  (Soderberg et al. 2004; Burrows et al. 2006; Grupe et al. 2006; Panaitescu 2006; Racusin et al. 2009). In the following, we set  $1/f_b = 15$ , corresponding to a half-opening angle  $\theta \simeq 20^\circ$  (Bartos et al. 2011). By taking into account all these factors, the merger rate  $R_{\text{merger}}(z)$  and the expected rate of SGRB observations  $R_{\text{SGRB}}(z)$  are

$$R_{\text{merger}}(z) = \frac{f_{\text{SGR}}}{T f_b f_{\text{FOV}} f_R} N'(z) \quad (6)$$

and

$$R_{\text{SGRB}}(z) = \frac{1}{T} N'(z), \quad (7)$$

respectively.

### 3. Results and Discussion

The results of our analysis are summarized in Table 2. The approximate local merger rate of binary compact objects ranges from 479 to 1025  $\text{Gpc}^{-3}\text{yr}^{-1}$ , depending on the chosen rate function. The upper limit comes from the model with unity rate function, which assumes no evolution on star formation over cosmological distances. The Porciani delayed rate function with delay times of 20 Myr and 100 Myr gives merger rates about 50% larger than without the delay. Extrapolating this result to the other functions, a reasonable estimate for the merger rate in the local universe is in the range  $\simeq 500$  to 1500  $\text{Gpc}^{-3}\text{yr}^{-1}$ . These results strongly depend on the half-opening angle of the SGRB jets. Figure 3 shows the dependence of the merger rate on the opening angle  $\theta$ . The smaller the angle, the larger is the number of mergers because the observer must be in the outflow cone to detect the SGRB. Assuming an half-opening angle of  $10^\circ$ , the merger rate could be as high as several thousand  $\text{Mpc}^{-3}\text{yr}^{-1}$ . A more isotropic large half-opening angle of  $60^\circ$  yields a rate of the order of 100  $\text{Mpc}^{-3}\text{yr}^{-1}$ .

Assuming that a satellite with a field-of-view comparable to the field of view of SWIFT is operating at the time of advanced GW detectors, and using the expected range for Advanced LIGO/Virgo (LIGO Scientific Collaboration and Virgo Collaboration 2010), we can estimate the number of coincident observations of SGRBs with GW counterparts. Under the above assumptions, we estimate about 0.2 to 1 coincident observations per year for a NS-NS mergers progenitor (detector range  $\simeq 450$  Mpc) and about 1 to 3 coincident observations per year for a NS-BH progenitor (detector range  $\simeq 930$  Mpc), a result consistent with earlier estimates (see Metzger & Berger (2012); Bartos et al. (2012) and references therein). These values include the systematic uncertainties underlying the

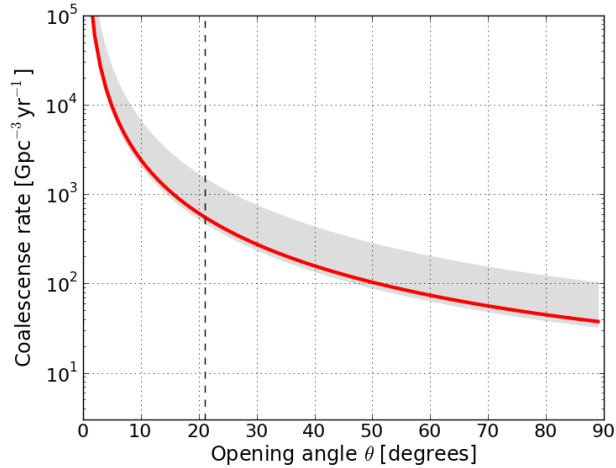


Fig. 3.— Merger rate of compact objects as a function of the half-opening angle  $\theta$ . The red line indicates the median result. The grey area spans the possible range of rates due to different fit models and systematic errors. The vertical dashed line indicates the typical opening angle which is used in our estimate.

estimates, as explained above. Since the advanced detectors are expected to operate for several years, a few observations of coincident SGRB-GW events seem likely.

These estimates could improve significantly with a network of operating GRB satellites. Assuming that Fermi<sup>2</sup> will be in operation during the advanced detector era, as well as the planned SVOM mission (Paul et al. 2011) and Lobster<sup>3</sup>, the coincident SGRB-GW detection rate could be higher than the above estimate by a factor  $\simeq 3$ . Ensuring that at least one GRB mission is operational at the time of advanced detectors will be crucial for

---

<sup>2</sup><http://fermi.gsfc.nasa.gov/>

<sup>3</sup>Neil Gehrels, private communication, 2011

identifying the host galaxy, measuring its redshift and star formation rate, and gaining valuable astrophysical information.

Our estimates can be compared to earlier published results which were obtained with alternative approaches. The two most common methods that are used to estimate the merger rate of compact objects rely on deriving the rates from observed pulsar observations (Kalogera et al. 2004) or employing population synthesis models (Belczynski et al. 2007). Both approaches inherit large statistical or systematic errors. A recent review article summarizes these results, concluding that the rate of merger events is somewhere between 10 and 10000  $\text{Gpc}^{-3}\text{yr}^{-1}$  (LIGO Scientific Collaboration and Virgo Collaboration 2010). Other investigations rely on methods that are more similar to the method used here. Guetta & Piran (2005) use a sample of 5 SGRBs to estimate a merger rate in the range 8-30  $\text{Gpc}^{-3}\text{yr}^{-1}$ . An earlier analysis by one of the authors which is based on a less restrictive data sample and neglects individual GRB luminosities, yields a much higher rate of about 7800  $\text{Gpc}^{-3}\text{yr}^{-1}$  (Dietz 2011). Finally, a recent study by Coward et al. (2012) uses a different method based on single GRB observations. In this approach, the maximum distance at which individual SGRBs can be detected by SWIFT is calculated and the results are then combined to estimate a final local rate of 0.16 to 1100  $\text{Gpc}^{-3}\text{yr}^{-1}$ . These results show that our estimates are consistent with, and confirm previous merger rate estimates. Future SGRB observations and improved statistics may further strengthen this conclusion.

This work is the result of a Research Experience for Undergraduates (REU) project by Carlo Enrico Petrillo at the University of Mississippi. C.E.P., A.D., and M.C. are partially supported by the National Science Foundation through awards PHY-0757937

and PHY-1067985. The authors would like to thank Jocelyn Read, Emanuele Berti, Maurizio Paolillo, Neil Gehrels and Richard O’Shaughnessy for their help and valuable comments. This publication has been assigned LIGO Document Number ligo-p1200015.

### A. Rate functions

This Appendix describes the various rate functions which are used in the analysis.

**Porciani.** The Porciani rate function is the SF2 function in Porciani & Madau (2001):

$$R(z) \propto \frac{\exp(3.4 z)}{\exp(3.4 z) + 22}. \quad (\text{A1})$$

**Hernquist.** The Hernquist rate function is (Hernquist & Springel 2003)

$$R(z) \propto \frac{\chi^2}{1 + \alpha(\chi - 1)^3 \exp(\beta\chi^{7/4})}, \quad (\text{A2})$$

where

$$H(z) = H_0 \sqrt{(1+z)^3 \Omega_M + \Omega_\Lambda}, \quad \chi(z) = \left[ \frac{H(z)}{H_0} \right]^{2/3}, \quad (\text{A3})$$

and  $\alpha = 0.012$ ,  $\beta = 0.041$ .

**Fardal.** The Fardal rate function is defined as (Fardal et al. 2007)

$$R(z) \propto \frac{a^{-p_2}}{(1 + p_1 a^{-p_2})^{p_3+1}} H(z) \quad (\text{A4})$$

where  $p_1 = 0.075$ ,  $p_2 = 3.7$ ,  $p_3 = 0.84$  and  $a = (1+z)^{-1}$ .

**Cole.** The Cole rate function is

$$R(z) \propto \frac{a + bz}{1 + (z/c)^d} H(z) \quad (\text{A5})$$

where the parameters are summarized for different authors in Table 3.

**Delayed functions.** Since the time between the formation of the compact objects and the merger of the binary system is typically of the order of the Gyr, the merger rate may not follow directly from the star formation rate. Assuming a delay with respect to the star formation rate, the delayed rate function is defined as

$$R_t(z) = \int_0^{t_d} dt \frac{1}{1 + z_f} R(z_{ret}) P(t), \quad (\text{A6})$$

where  $P(t)$  represents the probability distribution of the delay time. Population synthesis models (Belczynski et al. 2001; Postnov & Yungelson 2005) suggest that this distribution is a power law

$$P(t) \propto t^\alpha, \quad (\text{A7})$$

where  $\alpha \simeq -1$  for  $t > t_{\text{tmin}}$ . Although the observational literature has applied a much broader range of functional forms, a time delay probability distribution  $P(t) \sim 1/t$  is sufficient for the purposes of this analysis, where binaries are produced in the field<sup>4</sup>. The retarded redshift, i.e. the redshift at the time when the compact objects are formed, is

$$z_{\text{ret}} = T^{-1}(T(z) + t). \quad (\text{A8})$$

The lookback time at redshift  $z$  is (see, e.g., Hogg (1999))

$$T(z) = T_0 \int_0^{dz'} \frac{dz'}{(1 + z') \sqrt{(\Omega_k(1 + z')^3 + \Omega_k(1 + z')^2 + \Omega_\Lambda)}}. \quad (\text{A9})$$

---

<sup>4</sup>Richard O’Shaughnessy, private communication.

The expression in Eq. (A8) requires an integration and function inversion that in general need to be evaluated numerically. However, if flat cosmological models with  $\Omega_k = 0$  are considered, it is possible to obtain an analytic expression for the lookback time.

Substituting

$$v = \Omega_k(1+z)^3 \quad (\text{A10})$$

in Eq. (A8), the integral takes the form

$$T(z) = \frac{T_0}{3} \int_{v(0)}^{v(z)} dv' \frac{1}{v\sqrt{v + \Omega_\Lambda}}. \quad (\text{A11})$$

Integrating, it follows

$$T(z) = \frac{T_0}{3\sqrt{\Omega_\Lambda}} (L(v_0) - L(v_1)), \quad (\text{A12})$$

where

$$L(v) = \ln \left( \frac{\sqrt{v + \Omega_\Lambda} + \sqrt{\Omega_\Lambda}}{\sqrt{v + \Omega_\Lambda} - \sqrt{\Omega_\Lambda}} \right). \quad (\text{A13})$$

This analytic expression can be used to calculate the lookback time for a given redshift.

Solving Eq. (A12) for  $L(v_1)$ , we find

$$L(v_1) = L(v_0) - 3\sqrt{\Omega_\Lambda} \frac{T}{T_H} \equiv \ln E(T). \quad (\text{A14})$$

The value of  $L(v_0)$  does not depend on  $z$  or  $T$ . Equation (A14) is a function of  $\Omega_M$  and  $\Omega_\Lambda$ , as one can see from Eq. (A13) and Eq. (A10). Solving Eq. (A13) for  $z$ , one finally obtains

$$z(T) = \left( \frac{\Omega_\Lambda}{\Omega_M} \right)^{1/3} \left[ \left( \frac{1 + E(T)}{1 - E(T)} \right)^2 - 1 \right]^{1/3} - 1. \quad (\text{A15})$$

Table 1: List of the 14 SGRBs observed by SWIFT between 2004 and 2011 which pass our selection criteria. The table shows the observed fluences, the redshifts and the methods used to estimate the spectroscopic redshifts of the host galaxies. The fluence data are taken from Sakamoto et al. (2008) (first 7 SGBRs) and the Gamma-Ray burst Coordinated Network [[http://gcn.gsfc.nasa.gov/gcn3\\_archive.html](http://gcn.gsfc.nasa.gov/gcn3_archive.html)] (last 7 SGBRs: Barbier et al. (2007), Sato et al. (2007), Cummings et al. (2008), Ukwatta et al. (2009), Markwardt et al. (2010a), Markwardt et al. (2010b), Krimm et al. (2010), respectively). The unusual durations of the SGRB 061006 and 070714B are due to light curves with a short initial event followed by a softer extended event. They are classified as SGRBs (see Schady et al. (2006) and Barbier et al. (2007)). All SGRBs are preceded by an afterglow except 060502B, 060801 and 101219, however only one galaxy was present in the error circle for these SGRBs.

GRB	Duration [s]	$z$	type	Reference	Fluence [ $10^{-7}$ erg/cm <sup>2</sup> ]
050416	2.0	0.6535	emission	Cenko et al. (2005), Soderberg et al. (2007)	3.7±0.4
051221	1.4	0.5465	emission	Berger & Soderberg (2005), Soderberg et al. (2006)	11.5±0.4
060502B	0.09	0.287	absorption	Bloom et al. (2006), Bloom et al. (2007)	0.4±0.1
060801	0.5	1.131	emission	Cucchiara (2006), Berger et al. (2007)	0.8±0.1
061006	130	0.4377	emission	Berger et al. (2007)	14.2±1.4
061201	0.8	0.111	emission	Berger (2006), Stratta et al. (2007)	3.3±0.3
070429B	0.5	0.9023	emission	Perley et al. (2007), Cenko et al. (2008)	0.6±0.1
070714B	64	0.9225	emission	Graham et al. (2007), Cenko et al. (2008)	5.1±0.3
071227	1.8	0.384	emission	Berger et al. (2007), D’Avanzo et al. (2009)	2.2±0.3
080905	1.0	0.1218	emission	Rowlinson et al. (2010)	1.4±0.2
090510	0.3	0.903	emission	Rau et al. (2009), McBreen et al. (2010)	3.4±0.4
100117	0.3	0.92	emission	Fong et al. (2011)	0.9±0.1
100816	2.9	0.8049	absorption	Gorosabel et al. (2010)	20.0±1.0
101219	0.6	0.718	emission	Chornock & Berger (2011)	4.6±0.3



Table 2: Estimates of merger rates and number of detections per year for Advanced LIGO/Virgo. The detector reach is 450 Mpc for NS-NS binary systems and 930 Mpc for NS-BH binary systems. Results for different rate functions are shown. The Porciani20 and Porciani100 rate functions include delay times of 20 Myr and 100 Myr, respectively.

Rate function	Merger rate $\text{Gpc}^{-3}\text{yr}^{-1}$	NS-NS Detections $\text{yr}^{-1}$	NS-BH Detections $\text{yr}^{-1}$
Unity	1025	525	3456
Hernquist	816	393	2750
Fardal	580	238	1954
Cole	485	170	1634
Hopkins	506	188	1706
Wilkins	553	206	1866
Porciani	479	196	1614
Porciani20	729	326	2457
Porciani100	757	340	2552

Table 3: Parameters of the Cole rate function for different models in the literature.

Reference	a	b	c	d
Cole (Cole et al. 2001)	0.0166	0.1848	1.9474	2.6316
Hopkins (Hopkins & Beacom 2006)	0.0170	0.13	3.3	5.3
Wilkins (Wilkins et al. 2008)	0.014	0.11	1.4	2.2

## REFERENCES

- Acernese, F., et al. 2008, *Class. Quant. Grav.*, 25, 184001
- Band, D., Matteson, J., Ford, L., et al. 1993, *Astrophys. J.*, 413, 281
- Barbier, L., Barthelmy, S. D., Cummings, J., et al. 2007, *GRB Coordinates Network*, 6623, 1
- Barthelmy, S.D., B. L. C. J. e. 2005, *Space Science Reviews*, 120, 143
- Bartos, I., Brady, P., & Marka, S. 2012, arxiv, 1212.2289
- Bartos, I., Finley, C., & Marka, S. 2011, *PRL*, 107, 251101
- Belczynski, K., Bulik, T., Dominik, M., & Prestwich, A. 2011, arxiv, 1106.0397
- Belczynski, K., Dominik, M., Bulik, T., et al. 2010, *Astrophys. J. Lett.*, 715, L138
- Belczynski, K., Kalogera, V., & Bulik, T. 2001, *Astrophys. J.*, 572, 407
- Belczynski, K., Kalogera, V., Rasio, F. A., Taam, R. E., & Bulik, T. 2007, *Astrophys. J.*, 662, 504
- Belczynski, K., et al. 2006, *Astrophys. J.*, 648, 1110
- Berger, E. 2006, *GRB Coordinates Network*, 5952, 1
- Berger, E., Fox, D. B., Price, P., et al. 2007, *Astrophys. J.*, 664, 1000
- Berger, E., Morrell, N., & Roth, M. 2007, *GRB Coordinates Network*, 7154, 1
- Berger, E., & Soderberg, A. M. 2005, *GRB Coordinates Network*, 4384, 1

- Bloom, J. S., Perley, D., Kocevski, D., et al. 2006, GRB Coordinates Network, 5238, 1
- Bloom, J. S., Perley, D. A., Chen, H.-W., et al. 2007, ApJ, 654, 878
- Burrows, D. N., Grupe, D., Capalbi, M., et al. 2006, ApJ, 653, 468
- Cao, X.-F., Yu, Y.-W., Cheng, K., & Zheng, X.-P. 2011, Mon.Not.Roy.Astron.Soc., 416, 2174
- Cenko, S. B., Kulkarni, S. R., Gal-Yam, A., & Berger, E. 2005, GRB Coordinates Network, 3542, 1
- Cenko, S. B., Berger, E., Nakar, E., et al. 2008, arXiv, 0802.0874
- Chapman, R., Priddey, R. S., & Tanvir, N. R. 2008, MNRAS, 395, 1515
- Chornock, R., & Berger, E. 2011, GRB Coordinates Network, 11518, 1
- Cole, S., et al. 2001, Mon. Not. Roy. Astron. Soc., 326, 255
- Coward, D., Howell, E., Piran, T., et al. 2012, Mon.Not.Roy.Astron.Soc., 425, 1365
- Cucchiara, A. 2006, GRB Coordinates Network, 5470, 1
- Cummings, J., Barthelmy, S. D., Baumgartner, W., et al. 2008, GRB Coordinates Network, 8187, 1
- Dalal, N., Holz, D. E., Hughes, S. A., & Jain, B. 2006, Phys. Rev. D, 74, 063006
- D’Avanzo, P., Malesani, D., Covino, S., et al. 2009, A&A, 498, 711
- Del Pozzo, W. 2011, arxiv, 1108.1317

- Dietz, A. 2011, *Astron. Astrophys.*, 529, A97
- Eichler, D., Livio, M., Piran, T., & Schramm, D. N. 1989, *Nature*, 340, 126
- Ellis, J., Mavromatos, N., Nanopoulos, D., Sakharov, A., & Sarkisyan, E. 2006, *Astropart. Phys.*, 25, 402
- Fardal, M. A., Katz, N., Weinberg, D. H., & Dav'e, R. 2007, *Mon. Not. Roy. Astron. Soc.*, 379, 985
- Fiore, F., Guetta, D., Piranomonte, S., D'Elia, V., & Antonelli, L. A. 2007, *Astron. Astroph.*, 470, 515
- Flanagan, Éanna É., & Hinderer, T. 2008, *Phys. Rev. D*, 77, 021502
- Fong, W.-f., Berger, E., Chornock, R., et al. 2011, *Astrophys.J.*, 730, 26
- Gorosabel, J., Castro-Tirado, A. J., Tanvir, N., et al. 2010, *GRB Coordinates Network*, 11125, 1
- Graham, J. F., Fruchter, A. S., Levan, A. J., et al. 2007, *GRB Coordinates Network*, 6836, 1
- Grupe, D., Burrows, D. N., Patel, S. K., et al. 2006, *ApJ*, 653, 462
- Guetta, D., & Piran, T. 2005, *A&A*, 435, 421
- Guetta, D., & Stella, L. 2008, *A&A*, 498, 329
- Hernquist, L., & Springel, V. 2003, *Mon. Not. Roy. Astron. Soc.*, 341, 1253
- Hogg, D. W. 1999, [arXiv:astro-ph/9905116](https://arxiv.org/abs/astro-ph/9905116)

- Hopkins, A. M., & Beacom, J. F. 2006, *Astrophys. J.*, 651, 142
- Kalogera, V., et al. 2004, *Astrophys. J.*, 601, L179
- Keppel, D., & Ajith, P. 2010, *Phys. Rev.*, D82, 122001
- Kouveliotou, C., Meegan, C. A., Fishman, G. J., et al. 1993, *Astrophys. J.*, 413, L101
- Krimm, H. A., Barthelmy, S. D., Baumgartner, W. H., et al. 2010, *GRB Coordinates Network*, 11467, 1
- LIGO Scientific Collaboration and Virgo Collaboration. 2010, *Class. Quant. Grav.*, 27, 173001
- Markwardt, C. B., Barthelmy, S. D., Baumgartner, W. H., et al. 2010a, *GRB Coordinates Network*, 10338, 1
- . 2010b, *GRB Coordinates Network*, 11111, 1
- McBreen, S., Krühler, T., Rau, A., et al. 2010, *A&A*, 516, A71
- Metzger, B., & Berger, E. 2012, *Astrophys.J.*, 746, 48
- Nakar, E., Gal-Yam, A., & Fox, D. B. 2006, *Astrophys. J.*, 650, 281
- Narayan, R., Paczynski, B., & Piran, T. 1992, *Astrophys. J.*, 395, L83
- Nissanke, S., Holz, D. E., Hughes, S. A., Dalal, N., & Sievers, J. L. 2010, *Astrophys. J.*, 725, 496
- Panaitescu, A. 2006, *MON.NOT.ROY.ASTRON.SOC.LETT.*, 367, L42

- Panaiteescu, A., & Kumar, P. 2001, *Astrophys. J.*, 571, 779
- Pannarale, F., Tonita, A., & Rezzolla, L. 2010, *Apj*, 727, 95
- Paul, J., Wei, J., Basa, S., & Zhang, S.-N. 2011, *Comptes Rendus Physique*, 12, 298
- Perley, D. A., Bloom, J. S., Modjaz, M., Poznanski, D., & Thoene, C. C. 2007, *GRB Coordinates Network*, 7140, 1
- Piro, L. 2005, *Nature*, 437, 822
- Porciani, C., & Madau, P. 2001, *Astrophys. J.*, 548, 522
- Postnov, K., & Yungelson, L. 2005, *Living Rev. Rel.*, 9, 6
- Racusin, J. L., et al. 2009, *Astrophys. J.*, 698, 43
- Rau, A., McBreen, S., & Kruehler, T. 2009, *GRB Coordinates Network*, 9353, 1
- Read, J. S., Markakis, C., Shibata, M., et al. 2009, *Phys. Rev. D*, 79, 124033
- Rezzolla, L., Giacomazzo, B., Baiotti, L., et al. 2011, *ApjL*, 732, L6
- Rowlinson, A., et al. 2010, *Mon. Not. Roy. Astron. Soc.*, 408, 383
- Sakamoto, T., et al. 2008, *Astrophys. J. Suppl. Ser.*, 175, 179
- Sato, G., Barbier, L., Barthelmy, S. D., et al. 2007, *GRB Coordinates Network*, 7148, 1
- Schady, P., Burrows, D. N., Cummings, J. R., et al. 2006, *GRB Coordinates Network*, 5699, 1
- Smith, J. R. 2009, *Class. Quant. Grav.*, 26, 114013

- Soderberg, A. M., Kulkarni, S. R., Berger, E., et al. 2004, *Nature*, 430, 648
- Soderberg, A. M., Berger, E., Kasliwal, M., et al. 2006, *ApJ*, 650, 261
- Soderberg, A. M., Nakar, E., Cenko, S. B., et al. 2007, *ApJ*, 661, 982
- Stavridis, A., & Will, C. M. 2009, *Phys. Rev. D*, 80, 044002
- Stratta, G., D’Avanzo, P., Piranomonte, S., et al. 2007, *A&A*, 474, 827
- Ukwatta, T. N., Barthelmy, S. D., Baumgartner, W. H., et al. 2009, *GRB Coordinates Network*, 9337, 1
- Wilkins, S. M., Trentham, N., & Hopkins, A. M. 2008, *MNRAS*, 385, 687
- Will, C. M. 2005, *Living Rev. Rel.*, 9, 3